DOI: 10.1002/cssc.201100063

Glycerol Hydrogenolysis Promoted by Supported Palladium Catalysts

Maria Grazia Musolino, Luciano Antonio Scarpino, Francesco Mauriello, and Rosario Pietropaolo*[a]

Catalytic hydrogenolysis, with high conversion and selectivity, promoted by supported palladium substrates in isopropanol and dioxane at a low H_2 pressure (0.5 MPa), is reported for the first time. The catalysts, characterized by using BET isotherms, transmission electron microscopy (TEM), temperature-programmed reduction (TPR), powder X-ray diffraction (XRD), and X-ray photoelectron spectroscopy (XPS), were obtained by coprecipitation and impregnation techniques. The coprecipitation method allows catalysts with a metal–metal or a metal–support interaction to be obtained, which enhances the catalytic performance for both the conversion of glycerol and the selectivity to 1,2-propanediol. Analogous reactions carried out with catalysts prepared by using impregnation are less efficient. A study of the solvent and temperature effect is also presented. The obtained results allow the hydrogenolysis mechanism to be inferred; this involves both the direct replacement of the carbon-bonded OH group by an incoming hydrogen or the formation of hydroxyacetone as an intermediate, which subsequently undergoes a hydrogenation process to give 1,2-propanediol. Finally, catalytic tests on a large-scale reaction at a higher H_2 pressure and recycling of the samples were carried out with the better performing catalysts (Pd/CoO and Pd/Fe_2O_3 prepared by using coprecipitation) to verify possible industrial achievements.

Introduction

One of the most striking necessities of modern society is the development and the implementation of biofuels to overcome the dependence on petrol-based industry and to guarantee a more secure energy supply.[1] The most common first-generation biofuels are biodiesel and bioethanol. In recent years, over 200 major fleets of the United States (including the United States Post Office, the US Military, and the metropolitan transit systems) run on biodiesel, and Europe remains to be the leading biodiesel-producing region worldwide, with a landmark decision to introduce a 10% binding target for renewable energy use in transport.

Increasing biodiesel production by transesterification of plant oils and animal fats affords a large amount of glycerol as a byproduct. Therefore, it is the duty of chemistry to find a possible valorisation of the polyalcohol by exploring new routes to improve its commercial value.[2] Heterogeneous catalysis has been widely exploited to transform glycerol into intermediates for chemical production.[3] Interesting results have been obtained in different catalysis fields, such as reforming,[4] oxidation,[5] dehydration,[6] and etherification.[7]

In particular, the catalytic hydrogenolysis process leads to 1,2-propanediol (1,2-PDO) and 1,3-propanediol (1,3-PDO): the former is used mainly in manufacturing unsaturated polyester resins, functional fluids, cosmetics, pharmaceuticals, and so forth, whereas the latter is mainly used for the production of polyesters by copolymerisation with terephtalic acid.[2d] Different metal catalysts have been widely employed, such as copper,[8] ruthenium,[9] rhodium,[10] and platinum,[11] supported on a wide range of qualitatively different carriers and sometimes in the presence of Brønsted acids as co-catalysts. The use Brønsted acid as co-catalyst favors the formation of acrolein as an intermediate.[12]

Generally, supported noble-metal catalysts are more active than transition metal oxide catalysts, but the selectivity to propanediols is lower.[10a]

The main peculiarity of the many experiments carried out so far is the detection of hydroxyacetone (AC), as an intermediate, during the production of 1,2-PDO from glycerol. However, whereas it is easy to understand a dehydration process involving an ionic mechanism, leading to AC in the presence of Lewis or Brønsted acid supports, it is difficult to invoke the same mechanism in many other experiments carried out in the presence of graphite or inorganic oxides as carriers.

Furthermore, whereas supported copper, ruthenium, rhodium, platinum, and nickel catalysts have been widely studied as hydrogenolysis catalysts, palladium has been neglected and, if it has been used, it was found to be poorly efficient towards dihydroxy derivatives.[2d]

However, in principle, the activity of palladium-supported catalysts can be improved by using an appropriate preparation method based on the coprecipitation technique, which generally leads to a better interaction between metal and support than that observed when using the impregnation method.[13] Accordingly, recent studies have demonstrated that coprecipi-

[a] *Prof. M. G. Musolino, Dr. L. A. Scarpino, Dr. F. Mauriello, Prof. R. Pietropaolo*
Dipartimento MecMat, Facoltà di Ingegneria
Università Mediterranea di Reggio Calabria, Loc. Feo di Vito
89122 Reggio Calabria (Italy)
Fax: (+39) 0965 875248
E-mail: rosario.pietropaolo@unirc.it

tated palladium catalysts were very effective, with respect to the analogous catalysts obtained by impregnation, towards the reduction of aliphatic carbonyls[14] or in the aqueous-phase reforming of ethylene glycol (EG).[15]

The results were explained with an insightful remark on the electronic peculiarities of the catalysts mainly deriving from the palladium–support or palladium–metal interactions.

In a previous communication, we reported on the easy hydrogenolysis of glycerol in isopropanol using nominal 10% Pd/Fe_2O_3 as the catalyst in the absence of additional H_2; the source of hydrogen was the secondary alcohol dehydrogenated by the supported palladium.[16]

Herein, we report new results concerning the hydrogenolysis reaction of glycerol at a low H_2 pressure (0.5 MPa) by using supported palladium catalysts. The main aims were 1) to test the efficiency of supported palladium catalysts in the hydrogenolysis of glycerol, 2) to investigate the overall mechanism of the reaction, and 3) to compare the results obtained with the best performing catalysts, prepared by using the coprecipitation technique, with the analogous catalyst obtained by using the impregnation method. Furthermore, an additional study concerning the solvent effect on the conversion of glycerol and the selectivity to products is also included. Finally, the better performing catalysts were tested, on a large-scale reaction, at a higher H_2 pressure (4 MPa) to verify possible industrial achievements.

Results and discussion

Glycerol hydrogenolysis in an autoclave reactor

Conversion and selectivity data relative to the hydrogenolysis of glycerol in 2-propanol and dioxane in the presence of different coprecipitated and impregnated catalysts, previously reduced at 473 K for 2 h, are reported in Table 1. Values concerning PdCo and PdFe, in dioxane, attain to unactivated samples, since, if previously activated and then exposed to air, these catalysts easily ignite once poured into the solution.

Experiments performed at a low glycerol concentration (4 wt%) make it possible to obtain evidence on the influence of the nature of the support, the preparation method of the catalyst, and the solvent effect on the reactivity. The best conversion (100%) was achieved with PdCo and PdFe in 2-propanol as well as dioxane at 453 K. PdCo, at 423 K in 2-propanol, also afforded 100% conversion, compared to 75.1% conversion of PdFe, and can be considered to be the most efficient catalyst of the series (Figure 1). Other co-precipitated catalysts, PdNi and PdZn, evidence a good conversion (90.1 and 93.6%, respectively). Conversely, impregnated samples, $PdCo^I$ and $PdFe^I$, are less active (their conversion was 66.2 and 38.3%, respectively).

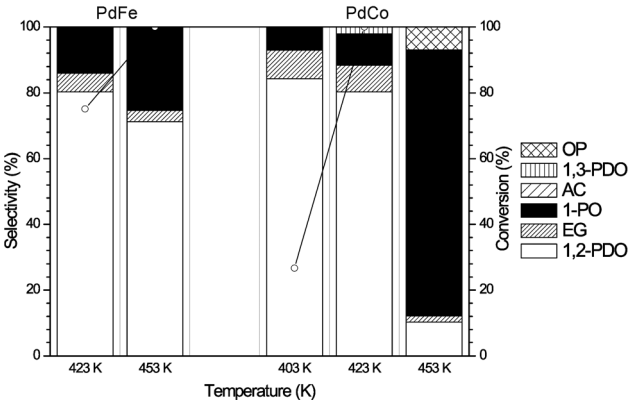

Figure 1. Temperature effect on glycerol hydrogenolysis over PdCo and PdFe catalysts. ○: glycerol conversion. Reaction conditions: 4 wt% glycerol solution in 2-propanol; initial H_2 pressure 0.5 MPa; reaction time 24 h.

Therefore, the activity changes in the order PdCo > PdFe > PdZn ≈ PdNi > $PdCo^I$ > $PdFe^I$ in 2-propanol.

A comparison of the values in Table 1 demonstrates that the hydroxylated and more polar 2-propanol favors the reaction more than the apolar dioxane.

Interestingly, in dioxane, the PdCo and PdFe catalysts, although unactivated, show a higher activity than the other activated samples.

Generally, 1,2-PDO was the main product and only a low selectivity to EG was obtained. However, the EG selectivity increased to 34.5%, at a conversion of about 66%, in the presence of $PdCo^I$. No or very low amounts of 1,3-PDO were detected; only PdZn afforded 6.3% 1,3-PDO in isopropanol. 1-propanol (1-PO) was also obtained as a reaction product and appeared to be the main product with the very reactive PdCo in both solvents at 453 K. AC was detected using PdZn, $PdCo^I$, and $PdFe^I$ and was confirmed as an intermediate in glycerol hydrogenolysis. Interestingly, these catalysts are known to be

Table 1. Glycerol hydrogenolysis promoted by supported palladium catalysts carried out at 453 K and 0.5 MPa H_2 pressure for 24 h.[a]

Catalyst	2-Propanol							Dioxane					
	Conversion	Selectivity [%]						Conversion	Selectivity [%]				
	[%]	1,2-PDO	EG	1-PO	AC	1,3-PDO	OP	[%]	1,2-PDO	EG	1-PO	AC	OP
PdCo	100	10.2	1.9	80.9	–	–	7.0	100[b]	60.0	–	30.5	–	9.5
PdFe	100	71.2	3.4	25.4	–	–	–	100[b]	72.4	3.0	22.9	1.7	–
PdZn	93.6	59.2	–	3.3	19.4	6.3	11.8	66.1	97.7	2.3	–	–	–
PdNi	90.1	84.5	10.1	–	5.4	–	–	80.1	79.5	13.3	–	7.2	–
$PdCo^I$	66.2	37.8	34.5	–	27.7	–	–	–	–	–	–	–	–
$PdFe^I$	38.3	26.1	4.9	–	69.0	–	–	–	–	–	–	–	–

[a] 1-PO = 1-propanol, OP = other products. [b] Unreduced sample.

poorly reactive towards carbonyl reduction under mild conditions (323 K and 0.1 MPa).[14]

It is worth noting the high conversion of glycerol to 1-PO when using PdCo and PdFe as catalysts in 2-propanol; this is at variance with the initial molar ratio of H_2/glycerol (≅1.6). However, it is useful to remember that H_2 can be also formed by dehydrogenation of 2-propanol. In many experiments acetone was, in fact, detected thus confirming the increase of the hydrogen content. We recently reported that coprecipitated 10% Pd/Fe_2O_3 catalyzed the reduction of glycerol in 2-propanol and in the absence of added hydrogen.[16]

The temperature effect on the conversion and selectivity of PdCo and PdFe in isopropanol is shown in Figure 1. As expected, the selectivity to 1-PO drastically decreased at 423 K, whereas that to 1,2-PDO (≈80%) increased. However, at 423 K the conversion of PdCo was very high (100%), whereas that of PdFe dropped to about 75%. PdCo maintained an appreciable conversion also at 403 K (≈25%). The combined results indicate the sequence of reactions reported in Scheme 1.

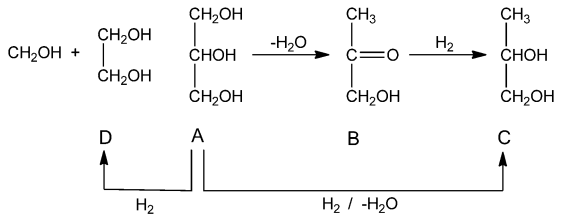

Scheme 1. Sequence of reactions for the conversion of glycerol.

Large-scale reactions and recycling of catalysts

The better performing catalysts, PdCo and PdFe, were also tested in a large-scale reaction (45 wt% of glycerol in isopropanol; initial molar ratio of H_2/glycerol ≅1) at 4 MPa initial pressure of H_2 (Table 2).

Table 2. Large-scale glycerol hydrogenolysis (45 wt% of glycerol in 2-propanol) carried out at 453 K for 24 h, with an initial H_2 pressure of 4 MPa.

Catalyst	Conversion [%]	Selectivity [%] 1,2-PDO	EG	1-PO	1,3-PDO
PdCo	70.7	86.5	9.2	2.6	1.7
PdFe	42.8	90.2	2.5	5.7	–

The best conversion (70.7%) after 24 h was obtained with PdCo (compared to 42.8% for PdFe). A good selectivity towards 1,2-PDO (86.5%) was also detected with PdCo, whereas that of PdFe was only 40.2%.

Further recycling of the PdCo catalyst, performed after washing the sample (remaining in the reactor) several times with 2-propanol, gave, as expected, a lower conversion (Figure 2). However, the selectivity did not change appreciably, as already reported for other catalysts.[17] Sintering, possible formation of impurities, and leaching of the metal from the catalyst may explain the decreased activity, although only small conversion changes occurred from the second to the fifth cycle. In any case, the reported data demonstrated the good potential for practical applicability of the coprecipitated Pd/CoO catalyst and provided evidence that palladium, when properly supported and prepared, was better than commercial products and could be a good catalyst for glycerol hydrogenolysis.

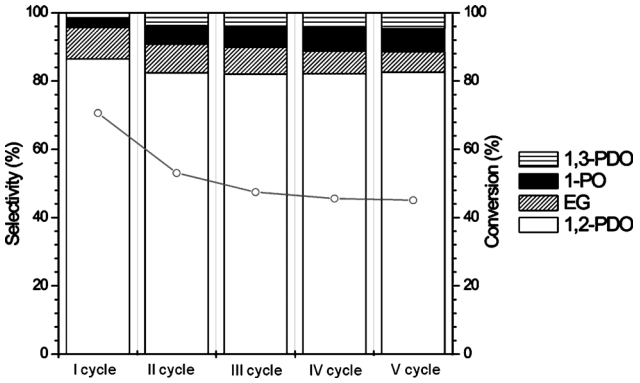

Figure 2. Re-use of the PdCo catalyst in the glycerol hydrogenolysis. ○: glycerol conversion. Reaction conditions: 45 wt% glycerol solution in 2-propanol; reaction temperature 453 K; initial H_2 pressure 4 MPa; reaction time 24 h.

Hydrogenolysis mechanism

The sequence of reactions in Scheme 1 raises the questions about 1) how the dehydration process A→B can occur in the absence of Brønsted or Lewis acids and 2) how C–OH bond breaking and C–H bond formation (substitution mechanism) can occur together with the dehydration process. In principle, both S_{N1}- and S_{N2}-type mechanisms may explain the palladium-catalyzed radical H/OH substitution at a carbon centre.[18]

We focus our attention on spectroscopic evidence in the literature[19] that, even though the O–H bond is several kJ mol^{-1} stronger than that of the C–H bond,[20] the C–O bond of alcohols is generally retained in mid to late transition metals, as consequence of the O–H bond breaking on the surface. An interesting consequence of a secondary alkoxide binding to a metal surface in a polyol molecule is that the metal–alkoxide bond can make it easier to break the adjacent C–OH bond through the neighboring group participation involving a Pd–H species.

This phenomenon is well known in organic and coordination chemistry[21] and can be transferred to catalytic surfaces. Specifically, such an event may occur in two possible ways (Scheme 2): 1) direct substitution of the carbon-bonded OH group by an incoming hydrogen to afford directly 1,2-PDO (Scheme 2b) or 2) interaction between a palladium-bonded hydrogen and a primary alcohol group leading to a vinylic alkoxide, which rapidly converts to a vinylic alcohol and then rearranges to AC through a keto–enol equilibrium (Scheme 2a). The quantitative ratio of both reactions depends on the relative activation energies and, therefore, on the nature of the

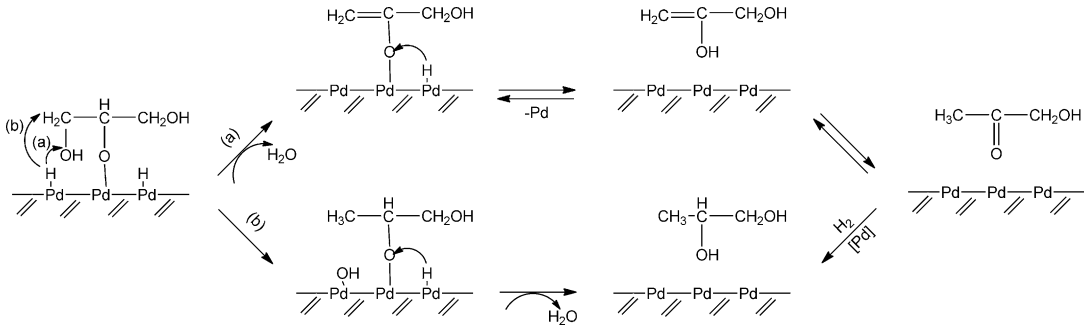

Scheme 2. Possible reaction pathways for alkoxide binding to a metal surface: a) Interaction between a palladium-bonded hydrogen and a primary alcohol; b) direct substitution of a carbon-bonded OH group by an incoming hydrogen.

catalyst. AC (Scheme 2a) further reacts with hydrogen to give 1,2-PDO as the product.

Catalysts characterization

The catalysts were characterized, whenever possible, by using nitrogen adsorption–desorption isotherms (BET), transmission electron microscopy (TEM), temperature-programmed reduction (TPR), powder X-ray diffraction (XRD), and X-ray photoelectron spectroscopy (XPS). Characterization using XRD and XPS measurements of the reduced PdCo sample could not be carried out, as the formation of small cobalt particles makes the catalyst unstable as soon as it is exposed to air.

Experimental loading, BET and TEM values of all the catalysts used are reported in Table 3. Micrographs of some representative catalysts and their relative particle distributions are shown in Figure 3. The PdCo catalyst showed a broad size distribution with a mean diameter of 10.7 nm; higher than the other coprecipitated samples that exhibited a predominance of small metallic particles and a relatively narrow particle size distribution. TEM microphotographs of CoO- and Fe_2O_3-supported palladium catalysts, prepared by impregnation, exhibited palladium particles dispersed on the matrix and also particle agglomeration spots. Moreover, for the $PdCo^{I}$ sample, a narrow particle size distribution centred around 4 nm was obtained, whereas for $PdFe^{I}$ particles in the range of 4–20 nm were observed.

Table 3. Main characteristics of the supported palladium catalysts tested.

Catalyst	Support	Pd loading [wt%] Nominal	XRF	S.A.[a] [$m^2 g^{-1}$]	d_n[b] [nm]
PdCo	CoO	5	3.7	106	10.7
PdFe	Fe_2O_3	5	8.7	170	2.4
PdZn	ZnO	5	5.2	85	2.7
PdNi	NiO	5	5.0	90	4.2
$PdCo^{I}$ [c]	CoO	5	4.5	8	4.3
$PdFe^{I}$ [c]	Fe_2O_3	5	5.5	6	7.1

[a] S.A. = surface area. [b] Mean particle size from TEM. [c] Catalysts prepared by the impregnation technique.

TPR patterns of all investigated catalysts are reported in Figure 4. The profiles of PdCo and PdNi are very similar and both show only a broad and intense peak, including palladium and simultaneously reduced cobalt or nickel. The main peculiarity of both patterns is that the reduction temperature shifts upward relative to that of palladium oxide[22] and downward relative to that of cobalt or nickel oxides (739 and 737 K, respectively).[14]

PdCo-supported catalysts have been extensively studied, and some structural aspects might have been settled at last.[23] In systems containing both palladium- and cobalt-supported oxides, the main peculiarities after calcination and subsequent H_2 reduction appear to be that 1) there is a strong promoting effect of palladium on cobalt oxide reduction (as also evidenced by our results); and 2) TPR experiments coupled with EDX analysis and magnetic measurements confirm that the particles contain both metals and EXAFS spectra emphasize the presence of alloys; the absence of any H_2 desorption confirms the result. Taking into account the reported literature, our results suggest that the H_2 reduction of the coprecipitated PdCo sample affords PdCo ensembles (possible alloys) and metallic cobalt. Furthermore, the TPR measurements carried out on PdCo and PdNi samples previously reduced at 473 K confirm the absence of any palladium β-hydride species on the bulk of the catalyst, as it may be expected if bimetallic ensembles are formed.

The TPR profile of PdZn evidences, as expected,[24] a peak at about 350 K due to the reduction of palladium cations, whereas the TPR profile of PdFe shows an intense peak at about 350 K, including both $Pd^{II} \rightarrow Pd^0$ and $Fe^{III} \rightarrow Fe_3O_4$ reductions, as deduced from the number of moles of H_2 absorbed.

Again, no negative peak, which could be attributed to β-hydride decomposition, is observed on the TPR spectrum of the PdFe sample pre-reduced at 473 K for 2 h, and this might suggest that a metal–support interaction occurs.[25] Figure 4 includes also TPR profiles of Pd/CoO and Pd/Fe_2O_3 prepared by impregnation. For both samples, the first peak refers to the $Pd^{2+} \rightarrow Pd^0$ reduction and is close to that of $[Pd(acac)_2]$ (acac = acetylacetonate), which is used as the precursor in the catalyst preparation.[14] The second peak attains to $Co^{2+} \rightarrow Co^0$ and $Fe_2O_3 \rightarrow Fe_3O_4$ reductions, respectively, and is weakly shifted towards lower temperatures with respect to that of pure oxides.

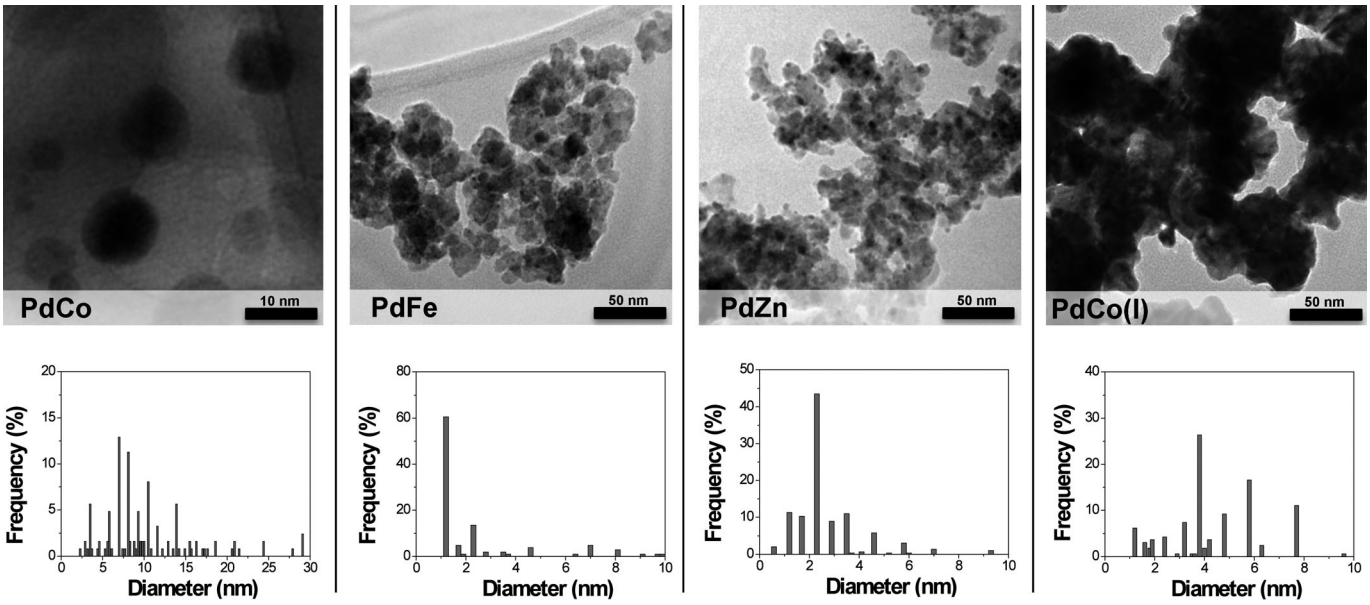

Figure 3. TEM microphotographs and metal particle size distribution histograms of the different supported palladium catalysts.

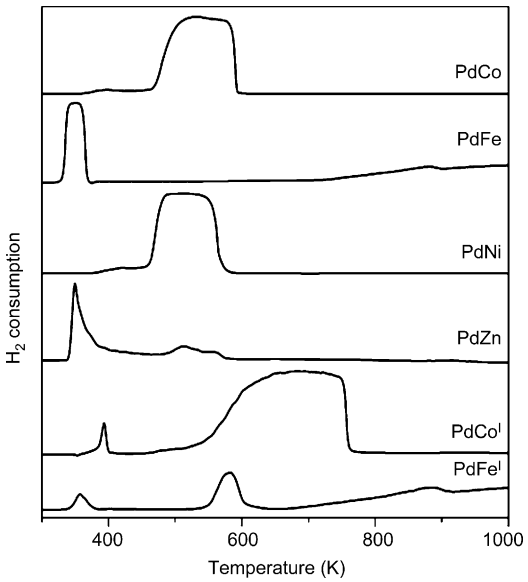

Figure 4. H_2-TPR profiles of the investigated palladium catalysts.

Decomposition of β-hydrides at 359 K for $PdCo^{I}$ is also observed. The results provide evidence that, in impregnated catalysts, only a weak or no interaction occurs between palladium and the supports. Conversely, TPR profiles of coprecipitated catalysts, with the exception of PdZn, may suggest that a metal–metal (PdCo and PdNi) or a metal–support interaction occurs.

XRD diffractograms of all palladium catalysts, except that of PdCo, after reduction at 473 K, are reported in Figure 5. Patterns referring to metal oxides carriers (NiO, ZnO, Fe_3O_4 on coprecipitated samples and CoO and Fe_2O_3 on impregnated catalysts) are easily detected. Furthermore, the peak located at $2\theta = 40.1^{\circ}$ is observed on all catalysts with the exception of PdNi and PdFe, corresponding to the most intense diffraction line of the (111) plane of metallic palladium. In particular, peaks

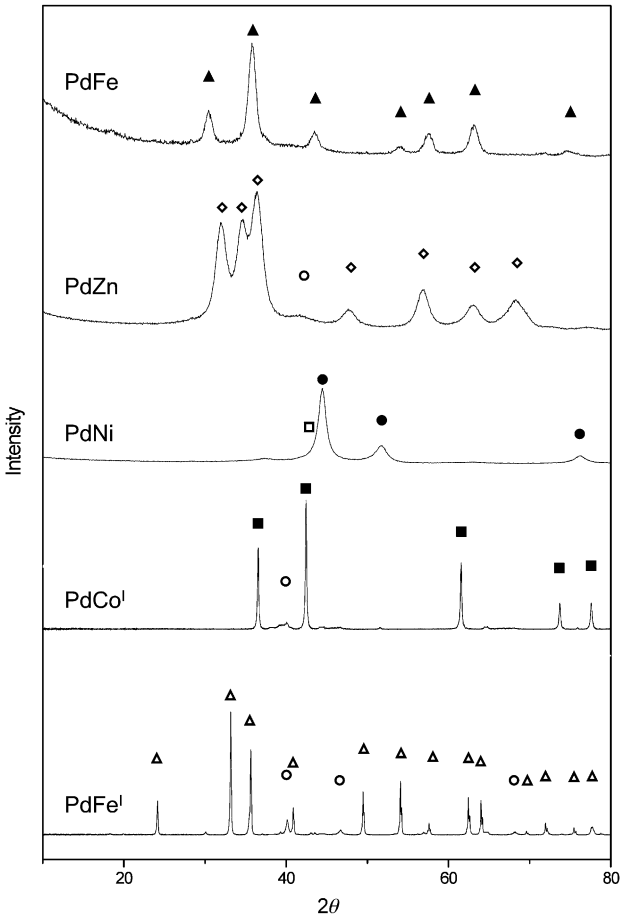

Figure 5. XRD patterns of the investigated palladium catalysts. ▲: Fe_3O_4; ◇: ZnO; □: NiO; ●: Ni, Pd(0.08)Ni(0.92); ●: CoO; △: Fe_2O_3; ○: Pd.

at $2\theta = 44.4$, 51.8, and 76.2° of PdNi, after deconvolution analysis, refer to both metallic nickel and a Pd(0.08)Ni(0.92) alloy.[14]

No palladium patterns were observed for PdFe. The most likely interpretation of this result stems, in our opinion, from the preparation technique used, which may influence the growth of palladium crystallites, probably embedded inside the support structure. Also on the basis of TEM and TPR observations, we may hypothesize that an intimate contact between palladium particles and the support, occurring in the first stage of their formation, leads to a palladium–support interaction that hinders crystallization and crystal growth of palladium particles. An identical conclusion was independently reached by other authors on the same coprecipitated sample,[15] suggesting that a strong metal–support interaction is responsible for the observed behavior. Binding energy values of reduced catalysts are summarized in Table 4. Values of 724.4 (Fe $2p_{1/2}$) and 710.9 eV (Fe $2p_{3/2}$) were obtained for PdFe. The absence of the satellite peak at about 718.8 eV indicates, as expected, a magnetite structure for the surface iron oxide support.[26]

Table 4. Binding energy values of reduced catalysts.

Catalyst	Binding energy [eV]						
	Pd $3d_{5/2}$	Co $2p_{3/2}$	Fe $2p_{3/2}$	Fe $2p_{3/2}$[a]	Fe $2p_{1/2}$	Zn $2p_{3/2}$	Ni $2p_{3/2}$
PdFe	335.2		710.9		724.4		
PdZn	334.9					1021.8	
PdNi	335.7						854.6
$PdCo^{I}$	334.8	780.2					
$PdFe^{I}$	334.8		710.4	718.4	723.8		

[a] Satellite peak.

The PdNi spectrum has a shoulder at 852.5 eV and a broad peak centered at 854.6 eV, both attributable to Ni $2p_{3/2}$; based on literature reports[27] the former is attributed to Ni^0 and the latter to Ni^{2+}. The Zn $2p_{3/2}$ spectrum of the PdZn sample displays a peak at about 1021.8 eV, in good agreement with the binding energy value reported for ZnO.[28] Impregnated catalysts are simple and easier to interpret. $PdFe^{I}$ has a peak (Fe $2p_{1/2}$) at 723.8 eV and that belonging to Fe $2p_{3/2}$ at 710.4 eV. The presence of the satellite shoulder at 718.4 eV indicates, in this case, a haematite structure.[26] $PdCo^{I}$ has a Co $2p_{3/2}$ peak at 780.2 eV, suggesting a CoO structure.[29]

Pd $3d_{5/2}$ binding energy values are reported in Table 4 and range from 335.7 eV for PdNi to 334.8–334.9 for $PdFe^{I}$, $PdCo^{I}$, and PdZn. Interestingly, the last values are very close to the value reported for Pd^0[30] and are in accordance with the TPR profiles, which evidence a definite reduction peak of palladium cations, and their XRD patterns, which show a peak at $2\theta = 40.1°$ distinctive for metal palladium. The combined results confirm a lack of palladium–support interaction.

On the other hand, the shift towards higher values, observed in the Pd $3d_{5/2}$ binding energy zone for PdNi and PdFe catalysts, can be attributed to a change in the electronic density of palladium as a consequence of metal–metal or metal–support interactions.[31] Accordingly, the TPR profiles of PdNi demonstrate that Pd–Ni particles are formed, whereas the quantitative analysis of H_2 consumption reveals that the reduction of palladium cations catalyses the reduction of $Fe_2O_3 \rightarrow Fe_3O_4$ in the PdFe substrate.

Understanding the nature of the active site and the catalytic activity

Physico-chemical properties of the catalysts (BET, TEM, TPR, XRD, and XPS) suggest different structural peculiarities that are useful for interpreting the link between the observed reactivity and the catalyst structure. In particular, XPS data indicate that $PdFe^{I}$, $PdCo^{I}$, and PdZn contain bare palladium particles on the surface and a weak or no interaction occurs between the metal and the support. In this case, the conversion follows the order $PdFe^{I} < PdCo^{I} \ll PdZn$, as expected if the diameter of the particles changes in the order $PdZn < PdCo^{I} < PdFe^{I}$, and/or the influence of the surface area ($PdZn \gg PdCo^{I} > PdFe^{I}$) play a fundamental role in determining the activity. Conversely, literature reports[23] for PdCo and XPS, XRD, and TPR values for PdFe and PdNi, which are included in this paper, indicate that bimetallic particles (PdCo and PdNi) or particles with strong metal–support interactions (PdFe) are formed.[23] In both cases, the ensuing electron density modification on palladium particles makes the catalytic reaction reported in Scheme 2 easier. However, the order of activity $PdCo > PdFe \gg PdNi$ does not meet the change of binding energy values ($PdNi > PdFe$). Therefore, the nature of the cometal (cobalt) or of the support (magnetite) may be synergically involved in the mechanism and constitutes an additional factor that contributes to further increasing the observed reactivity. On the other hand, the bimetallic promoting effect of rhenium on the catalytic performance of Ru/Al_2O_3, Ru/C, Ru/ZrO_2, and Rh/SiO_2 on the conversion of glycerol was reported.[32] In any case, the most apparent observation is that coprecipitated catalysts favor the hydrogenolysis of glycerol more than the corresponding impregnated substrates.

In conclusion, it is reasonable to attribute the enhancement of the catalytic activity observed in coprecipitated samples to the modified electronic properties of palladium nanoparticles obtained by an appropriate catalyst preparation method.

Conclusions

The reported results indicate that supported palladium systems are suitable catalysts for the hydrogenolysis of glycerol.

The best performance, in terms of conversion and selectivity to 1,2-PDO, was obtained with coprecipitated Pd/CoO and Pd/Fe_2O_3 catalysts in isopropanol and dioxane at 453 K and an H_2 pressure of 0.5 MPa. Analogous reactions carried out with Pd/CoO and Pd/Fe_2O_3 catalysts prepared by impregnation were observed to be less efficient. Furthermore, in 2-propanol, the activity changed in the following order $PdCo > PdFe > PdZn \approx PdNi > PdCo^{I} > PdFe^{I}$.

Our data suggest that high conversion and selectivity in the hydrogenolysis of glycerol can be easily obtained by choosing an appropriate preparation technique of the catalysts: in coprecipitated samples, a good palladium–support (metal) interaction favors a better performance. AC was detected by using

PdZn, PdNi, PdCo[I] and PdFe[I] catalysts, confirming that it is an intermediate in glycerol hydrogenolysis. Finally, the best performing samples (PdCo and PdFe) were tested on a large-scale reaction at a higher H_2 pressure (4 MPa). In addition, after several recycles, PdCo appeared to be an efficient catalyst suitable for use on an industrial scale.

Experimental Section

Catalyst preparation: Supported palladium catalysts were obtained by using two different techniques: coprecipitation and impregnation. Catalysts prepared by using the coprecipitation technique, with a nominal palladium loading of 5 wt%, were obtained from aqueous solutions of the corresponding inorganic precursors. Anhydrous palladium chloride (Fluka, purum, 60% palladium) was dissolved in HCl and cobalt(II) nitrate hexahydrate (Fluka, purity $\geq$99%), nickel(II) nitrate hexahydrate (Aldrich, purity 98%), zinc(II) nitrate hexahydrate (Aldrich, purity 98%), and iron(III) nitrate nonahydrate (Fluka, purity $\geq$98%) were added. The obtained aqueous metal salt solutions were added dropwise into a 1 M aqueous solution of Na_2CO_3. After filtration and washing until chloride was removed, samples were dried for 1 day under vacuum at 353 K and further reduced at 473 K for 2 h under a flow of hydrogen. In the Pd/CoO specimen, the formation of small cobalt particles made it unstable when exposed to air. Therefore, after the reduction treatment, contact with air was avoided as good as possible.
Nominal 5% Pd/CoO and Pd/Fe_2O_3 were also prepared by incipient wetness impregnation of the commercial supports CoO (Aldrich, $S_{BET}=7\ m^2g^{-1}$) and Fe_2O_3 (Sigma–Aldrich, $S_{BET}=4\ m^2g^{-1}$) with a solution of palladium(II) acetylacetonate (Aldrich, purity 99%) in acetone. After impregnation, the samples were dried for 1 day under vacuum at 353 K and further reduced at 473 K for 2 h under a flow of hydrogen.

Catalysts characterization: BET surface areas were determined by using N_2 adsorption–desorption isotherms at liquid nitrogen temperature using a Micromeritics Chemisorb 2750 instrument. The composition of the flow of gas was N_2/He = 30:70. Samples were outgassed under a flow of nitrogen for 1 h at 473 K before measurements were taken. The catalyst particle sizes and relative morphologies were analyzed by performing TEM measurements using a JEOL 2000 FX instrument operating at 200 kV and directly interfaced with a computer for real-time image processing. The specimens were prepared by grinding the reduced catalyst powder in an agate mortar and then suspending it in isopropanol. A drop of the suspension, previously dispersed in an ultrasonic bath, was deposited on a copper grid coated by a holey carbon film. After evaporation of the solvent, the specimens were introduced into the microscope column. Particle size distributions were obtained by counting several hundred particles visible on the micrographs on each sample. From the size distribution, the number average diameter was calculated: $d_n=\Sigma n_i d_i/n_i$ in which n_i is the number of particles of diameter d_i. TPR measurements were performed by using a conventional TPR apparatus. The dried samples (50 mg) were heated at a linear rate of 10 K min^{-1} from 298 to 1273 K in a 5 vol% of H_2/Ar mixture at a flow rate of 20 cm^3 min^{-1}. H_2 consumption was monitored by using a thermal conductivity detector (TCD). A molecular sieve cold trap (maintained at 193 K) and a tube filled with KOH, placed before the TCD, were used to block water and CO_2, respectively. The calibration of signals was done by injecting a known amount of H_2 into the carrier. XRD data were acquired at room temperature on a Philips X-Pert diffractometer by using the Ni β-filtered $Cu_{K\alpha}$ radiation ($\lambda=0.15418$ nm). Analyses were performed on samples reduced at 473 K for 2 h and registered in the 2θ range of 10–80° at a scan speed of 0.5° min^{-1}. Diffraction peaks were compared with those of standard compounds reported in the JPCDS Data File. XPS analysis was performed on reduced, at 473 K for 2 h, samples, by using a Physical Electronics GMBH PHI 5800-01 spectrometer, equipped with a monochromatic $Al_{K\alpha}$ X-ray source. The binding energy was calibrated by taking the C 1s peak (284.6 eV) as a reference.

Catalytic activity measurements: Glycerol hydrogenolysis was carried out in a 250 mL stainless-steel batch reactor (Parr instrument) equipped with an electronic temperature controller and a magnetic stirrer. The reaction was normally conducted at 453 K, 0.5 MPa of initial hydrogen pressure, with the catalyst (0.600 g) in dioxane or 2-propanol (50 mL) and added to a solution of glycerol (25 mL; 12 wt%), for 24 h, using a 500 rpm stirring speed (initial molar ratio H_2/glycerol $\cong$1.6). The reaction sequence was as follows: Once the reactor was loaded as reported above, it was heated at the reaction temperature and set aside for the time established. Then, the system was cooled and, when at room temperature, the liquid was analyzed. Product analysis was performed with a gas chromatograph (HP model 5890) equipped with a wide bore capillarity column (CP-WAX 52CB, 50 m, inner diameter 0.53 mm) and a flame ionization detector. When the experiments were carried out using a higher amount of glycerol (45 wt%, 50 mL isopropanol), 0.900 g of catalyst and a higher pressure (4 MPa) were used (initial molar ratio of H_2/glycerol $\cong$1). The conversion and selectivity of glycerol were calculated on the basis of Equations (1) and (2):

$$\text{glycerol conversion } [\%] = \frac{\text{moles of reacted glycerol}}{\text{moles of glycerol feed}} \times 100 \qquad (1)$$

$$\text{glycerol selectivity } [\%] = \frac{\text{moles of defined product}}{\text{moles of reacted glycerol}} \times 100 \qquad (2)$$

Keywords: glycerol · heterogeneous catalysis · hydrogenolysis · palladium · sustainable chemistry

[1] R. Luque, L. Herrero-Davila, J. M. Campelo, J. H. Clark, J. M. Hidalgo, D. Luna, J. M. Marinas, A. A. Romero, *Energy Environ. Sci.* **2008**, *1*, 542–564.
[2] a) M. Pagliaro, M. Rossi, *The Future of Glycerol (2nd Edition)*, Royal Society of Chemistry, Cambridge, **2010**; b) M. Pagliaro, R. Ciriminna, H. Kimura, M. Rossi, C. Della Pina, *Angew. Chem.* **2007**, *119*, 4516–4522; *Angew. Chem. Int. Ed.* **2007**, *46*, 4434–4440; c) A. Behr, J. Eilting, K. Irawadi, J. Leschinski, F. Lindner, *Green Chem.* **2008**, *10*, 13–30; d) C.-H. Zhou, J. N. Beltramini, Y.-X. Fan, G. Q. Lu, *Chem. Soc. Rev.* **2008**, *37*, 527–549, and references therein.
[3] a) M. Hara, *ChemSusChem* **2009**, *2*, 129–135; b) F. Jérôme, Y. Pouilloux, J. Barrault, *ChemSusChem* **2008**, *1*, 586–613.
[4] a) G. Nawaratna, S. Adhikari, R. E. Lacey, S. D. Fernando, *Energy Environ. Sci.* **2010**, *3*, 1593–1599; b) X. Zhu, T. Hoang, L. L. Lobban, R. G. Mallinson, *Chem. Commun.* **2009**, 2908–2910.
[5] a) E. Taarning, A. T. Madsen, J. M. Marchetti, K. Egeblad, C. H. Christensen, *Green Chem.* **2008**, *10*, 408–414; b) D. Wang, A. Villa, F. Porta, D. Su, L. Prati, *Chem. Commun.* **2006**, 1956–1958.
[6] a) S.-H. Chai, H.-P. Wang, Y. Liang, B.-Q. Xu, *Green Chem.* **2007**, *9*, 1130–1136; b) B. Katryniok, S. Paul, M. Capron, C. Lancelot, V. Bellière-Baca, P. Rey, F. Dumeignil, *Green Chem.* **2010**, *12*, 1922–1925; c) Y. Liu, H. Tüysüz, C.-J. Jia, M. Schwickardi, R. Rinaldi, A.-H. Lu, W. Schmidt, F. Schüth, *Chem. Commun.* **2010**, *46*, 1238–1240; d) M. O. Guerrero-Pérez, M. A. Bañares, *ChemSusChem* **2008**, *1*, 511–513.
[7] a) M. Clacens, Y. Pouilloux, J. Barrault, *Appl. Catal. A* **2002**, *227*, 181–190; b) Y. Gu, A. Azzouzi, Y. Pouilloux, F. Jérôme, J. Barrault, *Green Chem.* **2008**, *10*, 164–167; c) S. Pariente, N. Tanchoux, F. Fajula, *Green Chem.* **2009**, *11*, 1256–1261.

[8] a) M. A. Dasari, P.-P. Kiatsimkul, W. R. Sutterlin, G. J. Suppes, *Appl. Catal. A* **2005**, *281*, 225 – 231; b) S. Wang, H. Liu, *Catal. Lett.* **2007**, *117*, 62 – 67.
[9] a) D. G. Lahr, B. H. Shanks, *J. Catal.* **2005**, *232*, 386 – 394; b) T. Miyazawa, Y. Kusunoki, K. Kunimori, K. Tomishige, *J. Catal.* **2006**, *240*, 213 – 221; c) T. Miyazawa, S. Koso, K. Kunimori, K. Tomishige, *Appl. Catal. A* **2007**, *318*, 244 – 251.
[10] a) J. Chaminand, L. Djakovitch, P. Gallezot, P. Marion, C. Pinel, C. Rosier, *Green Chemistry* **2004**, *6*, 359 – 361; b) I. Furikado, T. Miyazawa, S. Koso, A. Shimao, K. Kunimori, K. Tomishige, *Green Chem.* **2007**, *9*, 582 – 588.
[11] E. P. Maris, R. J. Davis, *J. Catal.* **2007**, *249*, 328 – 337.
[12] a) A. Alhanash, E. F. Kozhevnikova, I. V. Kozhevnikov, *Catal. Lett.* **2008**, *120*, 307 – 311; b) A. Alhanash, E. F. Kozhevnikova, I. V. Kozhevnikov, *Appl. Catal. A* **2010**, *378*, 11 – 18.
[13] a) F. Schüth, M. Hesse, K. K. Unger in *Handbook of Heterogeneous Catalysis* (Eds.: G. Ertl, H. Knozinger, F. Schüth, J. Weitkamp), Wiley-VCH, Weinheim, **2008**, p. 100; b) F. Liu, S. P. Xu, L. Cao, Y. Chi, T. Zhang, D. F. Xue, *J. Phys. Chem. C* **2007**, *111*, 7396 – 7402; c) G. Neri, G. Rizzo, L. De Luca, A. Donato, M. G. Musolino, R. Pietropaolo, *Appl. Catal. A* **2009**, *356*, 113 – 120; d) B. Bridier, N. López, J. Pérez-Ramírez, *J. Catal.* **2010**, *269*, 80 – 92.
[14] M. G. Musolino, C. Busacca, F. Mauriello, R. Pietropaolo, *Appl. Catal. A* **2010**, *379*, 77 – 86.
[15] J. Liu, B. Sun, J. Hu, Y. Pei, H. Li, M. Qiao, *J. Catal.* **2010**, *274*, 287 – 295.
[16] M. G. Musolino, L. A. Scarpino, F. Mauriello, R. Pietropaolo, *Green Chem.* **2009**, *11*, 1511 – 1513.
[17] J. Zhou, L. Guo, X. Guo, J. Mao, S. Zhang, *Green Chem.* **2010**, *12*, 1835 – 1843.
[18] a) N. Thakar, N. F. Polder, K. Djanashvili, H. van Bekkum, F. Kapteijn, J. A. Moulijn, *J. Catal.* **2007**, *246*, 344 – 350; b) M. G. Musolino, C. Busacca, C. V. Caia, F. Mauriello, R. Pietropaolo, unpublished results.
[19] a) X. Xu, C. M. Friend, *Surf. Sci.* **1992**, *260*, 14 – 22; b) M. K. Weldon, C. M. Friend, *Chem. Rev.* **1996**, *96*, 1391 – 1412.
[20] a) F. A. Carey, R. J. Sundberg, *Advanced Organic Chemistry A*, 3rd ed., Plenum, New York, **1990**; b) *Handbook of Chemistry and Physics* (Ed.: D. R. Lide), 73rd ed., CRC Press, Boca Raton, **1992**.
[21] M. B. Smith, J. March, *Advanced Organic Chemistry*, 4th Edition, Wiley, New York, **2001**.
[22] A. F. Gusovius, T. C. Watling, R. Prins, *Appl. Catal. A* **1999**, *188*, 187 – 199.
[23] a) F. B. Noronha, M. Schmal, R. Fréty, G. Bergeret, B. Moraweck, *J. Catal.* **1999**, *186*, 20 – 30; b) F. B. Noronha, M. Schmal, B. Moraweck, P. Delichère, M. Brun, F. Villain, R. Fréty, *J. Phys. Chem. B* **2000**, *104*, 5478 – 5485; c) C. Montes de Correa, F. Córdoba Castrillón, *Appl. Catal,. A* **2005**, *228*, 267 – 273.
[24] Y.-H. Chin, R. Dagle, J. Hu, A. C. Dohnalkova, Y. Wang, *Catal. Today* **2002**, *77*, 79 – 88.
[25] S. Subramanian, J. A. Schwarz, *J. Catal.* **1991**, *127*, 201 – 212.
[26] a) M. Muhler, R. Schlögl, G. Ertl, *J. Catal.* **1992**, *138*, 413 – 444; b) T. Yamashita, P. Hayes, *Appl. Surf. Sci.* **2008**, *254*, 2441 – 2449.
[27] a) K. Hadjiivanov, M. Mihaylov, D. Klissurski, P. Stefanov, N. Abadjieva, E. Vassileva, L. Mintchev, *J. Catal.* **1999**, *185*, 314 – 323; b) J.-G. Kim, D. L. Pugmire, D. Battaglia, M. A. Langell, *Appl. Surf. Sci.* **2000**, *165*, 70 – 84.
[28] K. Dumbuya, R. Deneke, H.-P. Steinrück, *Appl. Catal. A* **2008**, *348*, 209 – 21327.
[29] T. J. Chuang, C. R. Brundle, D. W. Rice, *Surf. Sci.* **1976**, *59*, 413 – 429.
[30] a) M. L. Cubeiro, J. L. G. Fierro, *J. Catal.* **1998**, *179*, 150 – 162; b) N. Iwasa, S. Masuda, N. Ogawa, N. Takezawa, *Appl. Catal. A* **1995**, *125*, 145 – 157.
[31] K. Sun, W. Lu, M. Wang, X. Xu, *Appl. Catal. A* **2004**, *268*, 107 – 113.
[32] a) L. Ma, D. He, Z. Li, *Catal. Commun.* **2008**, *9*, 2489 – 2495; b) Y. Shinmi, S. Koso, T. Kubota, Y. Nakagawa, K. Tomishige, *Appl. Catal. B* **2010**, *94*, 318 – 326.

Received: February 1, 2011
Published online on June 28, 2011

